Control of localized structures in an optical feedback interferometer

P. L. Ramazza, S. Boccaletti,[a] U. Bortolozzo, and F. T. Arecchi[b]
Istituto Nazionale di Ottica Applicata, Largo E. Fermi, 6, I50125 Florence, Italy

(Received 14 March 2002; accepted 2 August 2002; published 21 February 2003)

We report a detailed experimental investigation of the dependence of localized structures, observed in a nonlinear optical device, on several control parameters. A first step of the study consists in the determination of the region of existence of localized states as a function of the system variables. Subsequently, we show how different control parameters can be used to the aim of tuning several localized structures properties; among these, of particular relevance are the contrast and the amplitude and frequency of the oscillations appearing on the tails of the structures. A discussion of the relation between the localized states here studied and the one predicted by general model for pattern forming systems is also given. © *2003 American Institute of Physics.*
[DOI: 10.1063/1.1513137]

During the last two decades, the study of pattern formation and competition in spatially extended systems driven out of thermodynamical equilibrium has been extensively carried out.[1] Among the different fields wherein these investigations have been performed, nonlinear optics represents a fruitful area of activity. This is due to the fact that patterned states arises naturally from the interplay of diffraction, optical nonlinearities, and other physical mechanisms in many optical devices.[2,3] In this context, special attention has been recently paid to the emergence of localized states. Aside the fundamental interest in the phenomenon of localization that these states stimulate, optical solitary structures are considered promising in view of applications as pixels in image processing systems. Here we report a detailed characterization of optical localized structures observed in a nonlinear optical interferometer. We delimit the existence range of these structures in the parameter space, and give evidence of the broad possibility of tuning the main features of an individual localized structure by means of external control variables.

I. INTRODUCTION

Localized structures can be loosely defined as structures that appear to be concentrated in delimited regions of the spatial domain available for a given system, as opposed to delocalized patterns that cover it entirely. Many analytical and numerical works have pointed out the several different mechanisms that can lead to localization of patterns in dissipative systems.[4] Simultaneously, experimental observations of localized structures have been offered in different fields, such as fluid dynamics,[5] chemistry,[6] granular materials,[7] and nonlinear optics.[8–14] Namely, in this last framework, optical localized structures have been observed in photorefractive cavities,[8,9] in passive nonlinear feedback interferometers,[10–12] and in microresonators filled with semiconductor media.[13,14] Furthermore, localized structures (LS) are currently object of intense researches, in view of possible applications as optical pixels in devices for information storage or processing. To this purpose, however, crucial issues such as the control of their shapes and their interactions by means of accessible parameters have not been extensively addressed so far.

In this paper, we focus on the appearance of LS in a nonlinear optical interferometer, and discuss the modifications of these structures observed in response to the variation of several external control parameters. These parameters provide a sensitive tool to control the most important features of the localized structures, including their stability, shape, and interaction properties.

II. PINNING INDUCED LOCALIZED STRUCTURES

Among the several mechanisms of pattern localization that have been unambiguously identified,[4] pinning of the fronts connecting different states of the system is the one operating in our experiment (Secs. III and IV). This phenomenon takes place in the presence of a subcritical bifurcation of a uniform solution toward a patterned state.[15,16] In these conditions, a region of bistability exists, where both the uniform and the patterned branches of the bifurcation are stable. Therefore, a proper localized, finite amplitude perturbation applied to the stable uniform solution can generate a localized structure formed by a given number of cells of the patterned state. Thus LS result from the spatial pinning of the two stable solutions.

Analytical studies in one spatial dimension have approached this problem, showing that an infinite set of LS can be expected,[15,17] constituted by an increasing number of elementary cells of the patterned state.[18] To give an example of the above mechanism, we refer to the subcritical Swift–Hohenberg equation for a real order parameter u, that reads[16]

$$\frac{\partial u}{\partial t} = -u + \beta u^2 - u^3 - (q_c^2 + \nabla)^2 u, \tag{1}$$

[a]Also at Department of Physics and Applied Mathematics, Universidad de Navarra, Irunlarrea s/n, 31080 Pamplona, Spain.
[b]Also at Department of Physics, University of Florence, Florence, Italy.

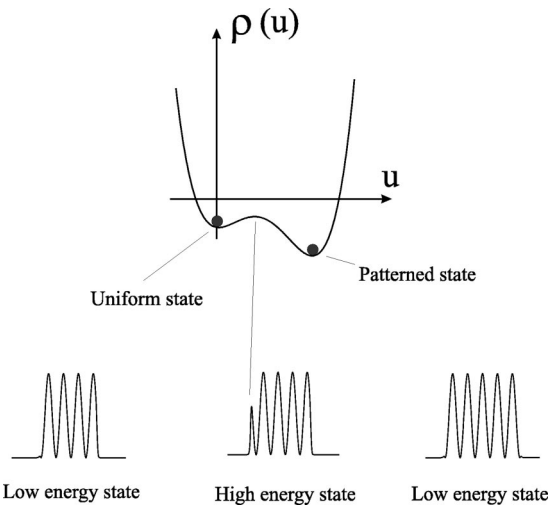

FIG. 1. Upper: Density of free energy associated to the stationary solutions of Eq. (1). Lower: Example of how the passage from one low energy state of the system to another requires transition trough an high-energy state.

where β is a real positive parameter and q_c represents the spatial wave number at which the patterned state bifurcates. Equation (1) can be written in a potential form as $\partial u/\partial t \equiv -(\partial V/\partial u)$, with V given by

$$V(u) = \int \{ \tfrac{1}{2}u^2 - \tfrac{1}{3}\beta u^3 + \tfrac{1}{4}u^4 + \tfrac{1}{2}[(q_c^2+\nabla^2)u]^2 \} dx \equiv \int \rho(u) dx, \quad (2)$$

where $\rho(u)$ is the free energy density of the system.

A schematic drawing of $\rho(u)$ versus u is given in Fig. 1. For a certain interval of values of β, this function has two minima, corresponding respectively to the uniform state with zero amplitude, and to a finite amplitude state spatially modulated at a frequency q_c. In these conditions, states of the system formed by an integer number of elementary cells of the modulated state, connected to the uniform state by a rather sharp interface, can be stable, giving rise to localization of the pattern over a finite region. An intuitive understanding of this phenomenon can be grasped by inspection of Fig. 1, which refers to a one-dimensional geometry. In order to pass from the low-energy configuration shown at the lower left corner to the other low-energy configuration shown at right, the system needs to cross at some time a state of the kind shown in the middle; this is a high-energy one, since part of the space, namely the interface between the uniform and the modulated regions, is in a state corresponding to the maximum of the energy density shown. Notice that the double well potential of Fig. 1 refers to homogeneous, infinitely extended states, so that the evaluation of localized patterns based on this picture has only a qualitative meaning.

In the context of model (1) or in others belonging to the same class, low amplitude oscillations in the spatial region connecting the two states giving rise to the localized structure have also been predicted.[16,23] This region is usually referred to as the ''tail'' of the localized structure. In two dimensions, the above oscillations give to each LS the shape of a central peak of high intensity, surrounded by a set of concentric rings of decreasing amplitude for increasing distance from the center. Experimental observations of this kind of structures have been reported, e.g., in granular materials[7] and in nonlinear optics.[10]

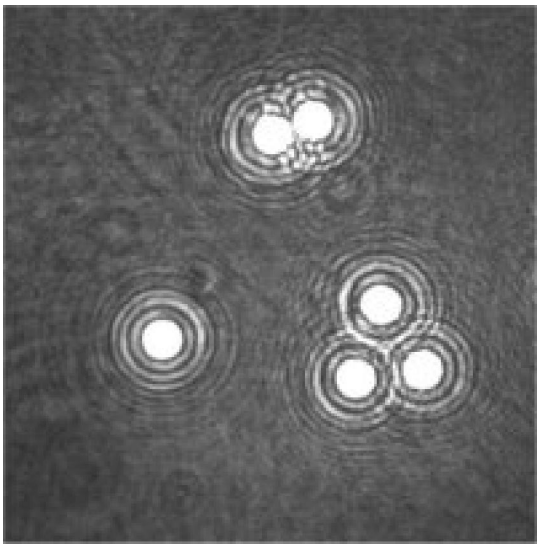

FIG. 2. Examples of a single localized structure and of bound states. Notice the difference in the distance between LS in the case of the binary and ternary states. These distances are not uniquely determined, and can be controlled by external parameters (Ref. 25).

The oscillations on the tails, which arise from the existence of weakly damped modes, lead to peculiar interactions between LS. In particular, the force between a pair of structures is of oscillating sign depending on their distance; as a consequence, molecule-like states formed by two or more bounded LS are possible. Examples of these bound states observed in our experiment are shown in Fig. 2. Their occurrence, first reported in a vibrated granular medium experiment,[7] has been recently object of investigations in nonlinear optical systems.[11,25] In particular, it has been shown how the properties of bound states can be tuned to a large extent by means of external control parameters.

III. LOCALIZED STRUCTURES IN THE LIQUID CRYSTAL LIGHT VALVE WITH FEEDBACK

The above scenario of bifurcations is realized by a liquid crystal light valve (LCLV) inserted in an optical feedback loop, in which both diffractive and interferential effects are present. The experimental setup is depicted in Fig. 3. The LCLV is formed by a nematic liquid crystal (LC) cell, followed by a mirror and a layer of photoconductive material.[19] A voltage of rms amplitude V_0 and frequency ν is applied to the series of these three elements. When the LCLV is inserted into an optical feedback loop, the fraction V_{LC} of voltage that falls across the LC cell is determined by both V_0 and the light intensity I_{fb} fed back on the photoconductive layer. Under the effect of V_{LC}, the LC reorients, thus inducing a space dependent phase retardation on a homogeneous input beam injected into the optical system. For a broad parameter range, the phase retardation can be considered proportional

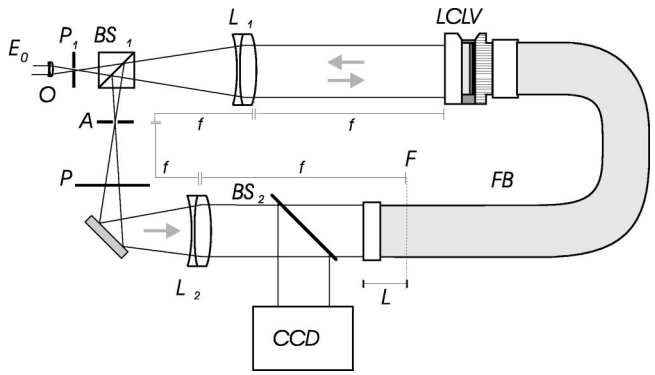

FIG. 3. Experimental setup. E_0 = input field; O = microscope objective; P_1 = pinhole; A = iris; BS_1, BS_2 = beamsplitters; LCLV = liquid crystal light valve; L_1, L_2 = lenses of focal length f; P = polarizer; FB = fiber bundle; CCD = videocamera; F = image plane of the LCLV. The overall free propagation of a negative distance L results in a change of the system nonlinearity from self-defocusing, as it would be for the LCLV alone, to self-focusing. In the experiments here reported, $L = 25$ cm.

to I_{fb}. In the jargon of nonlinear optics, this amounts to say that, in the closed loop configuration, the LCLV operates as a Kerr-type medium.

Pattern forming instabilities have been studied in this system using several feedback configurations,[20–22] in order to identify the role of different physical mechanisms (diffraction, diffusion, nonlocal interactions, etc.) in determining the observed selection of patterns. Here we concentrate on an experimental setup that includes both diffraction and interference in the feedback path.

Precisely, diffraction is controlled by lenses L_1 and L_2 inserted within the system, and by the position of the plane F corresponding to the input of the fiber bundle; interference between the components of the light polarized parallel and perpendicular to the optical axis of the liquid crystals is obtained by means of their projection onto the transmissive axis of the polarizer P. Under these conditions, the equation governing the space time evolution of the phase $\varphi(\mathbf{r},t)$ induced by the LC on the input beam is[24]

$$\tau\frac{\partial\varphi(\mathbf{r},t)}{\partial t}=-(\varphi(\mathbf{r},t)-\varphi_0)+l_d^2\nabla_\perp^2\varphi(\mathbf{r},t)+\alpha I_{\mathrm{fb}}. \tag{3}$$

Here, $\varphi_0\equiv\varphi_0(V_0,\nu)$ is the space and time independent phase retardation induced by the LCLV in the absence of feedback intensity, l_d is the diffusion length of the liquid crystals, and α gives the sign and strength of the Kerr nonlinearity. Furthermore, the feedback intensity I_{fb} is given by

$$\begin{aligned}I_f&=I_0|e^{-(iL\nabla^2/2k_0)}(Be^{-i\varphi}+C)|^2\\&=B^2e^{(iL\nabla^2/2k_0)}e^{-i\varphi}e^{(iL\nabla^2/2k_0)}e^{i\varphi}\\&\quad+BC(e^{(iL\nabla^2/2k_0)}e^{-i\varphi}+e^{(iL\nabla^2/2k_0)}e^{i\varphi})+C^2.\end{aligned} \tag{4}$$

The diffraction operator $e^{-(iL\nabla^2/2k_0)}$ expresses in a formal way the fact that transverse Fourier components of the electric field at frequency q undergoes, by free propagation, a phase retardation $Lq^2/2k_0$ with respect to the on-axis field.

In Eq. (4), $I_0=|E_0|^2$ represents the linearly polarized input beam intensity, L is the free propagation length along the optical path, $k_0=2\pi/\lambda$ is the optical wave number, and the parameters B and C are given by

$$B=\cos\theta_1\cos\theta_2,\quad C=\sin\theta_1\sin\theta_2, \tag{5}$$

θ_1,θ_2 being, respectively, the angles formed by the input light polarization direction and by the polarizer P transmissive axis with the LC optical axis. In the following we specify to the case $\theta_1=\theta_2\equiv\theta$, so that $B=\cos^2\theta$, $C=\sin^2\theta$.

It is apparent from Eq. (3) that the system has several control parameters; here we focus our attention on (θ,I_0,V_0,q_b), where θ, I_0 and V_0 have been previously defined and q_b is the spatial frequency bandwidth, controlled by means of an iris A in the Fourier plane. We express q_b in units of the diffractive wave number $q_{\mathrm{diff}}=\sqrt{\pi k_0/L}$, that is

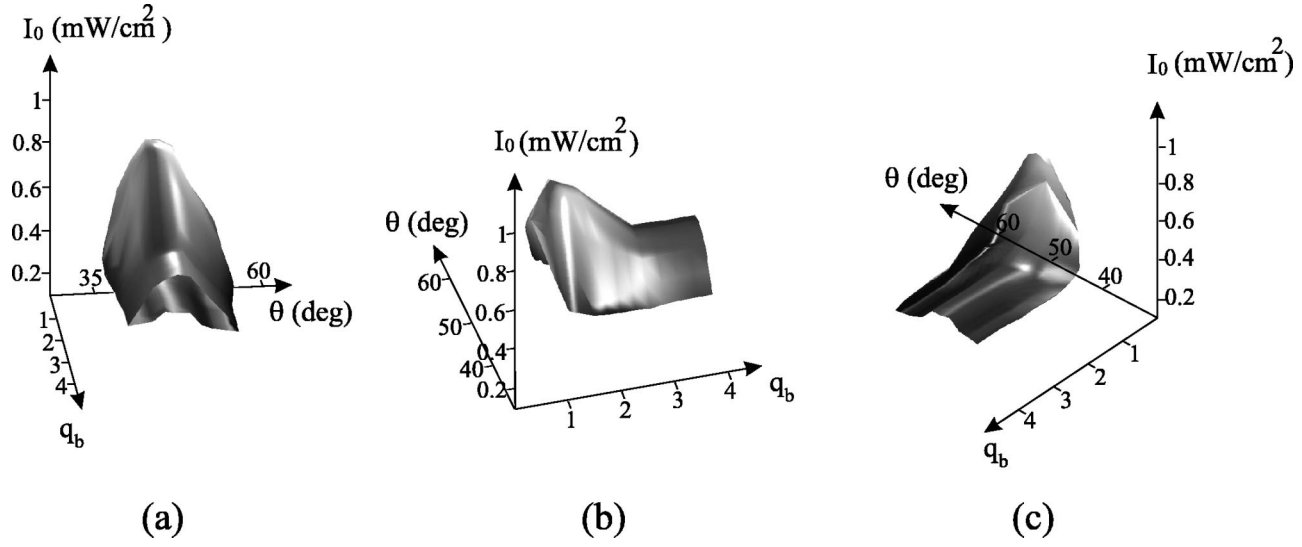

FIG. 4. Region of existence of the localized structures in the (q_b,θ,I_0) parameter space. The same data are visualized from three different perspectives. The value of φ_0 is kept fixed at 1.09π. All the data have been obtained by starting the observation at high values of intensity, and then gradually decreasing it.

the scale at which the system would patternize in the case of purely diffractive feedback, in the absence of diffusion.

We investigate the range of existence of localized structures. The necessary condition of coexistence of a lower uniform and an upper patterned branch is satisfied for a limited, though broad, range of parameters. Some information about this point can be gained by the linear stability analysis of the homogeneous uniform solutions for the phase φ.[12,24]

First we notice that, at any value of the triplet (θ, I_0, q_b), localization of patterns exists for a rather limited range of V_0, corresponding to φ_0 close to π. Only in this situation, indeed, the required bistability between a low intensity uniform state and an high-intensity patterned one is realized. When φ_0 differs from π by an amount larger than $\simeq 15\%$, the lower branch loses its stability with a supercritical bifurcation leading to other kinds of patterns, so that one of the conditions for localization of structures, namely bistability, is no longer met.

For all the measurements reported in this section, φ_0 has been held fixed at $1.09\,\pi$. In these conditions, (q_b, θ, I_0) are scanned as described below. Initially (q_b, θ) are kept fixed and the system is on the high-intensity patterned branch. At this point I_0 is decreased, leading to the formation of LS, which at smaller intensities die out, leaving the system in the lower homogenous state. It is to be stressed that the inverse procedure, consisting of an increase of I_0 starting from the homogeneous value, leads to the emergence of delocalized patterns via a subcritical bifurcation. Hence, as it is natural in the presence of the present scenario, the occurrence of localization depends on the system parameter history.

By scanning (q_b, θ) and repeating the above procedure, we map the volume of existence of the LS displayed in Fig. 4. It is seen here that the formation of LS is not limited to few particular values of the parameters, but is observed for over broad ranges of (q_b, θ, I_0) as a robust phenomenon.

Let us consider in particular the section of the existence volume in the planes parallel to (q_b, I_0), shown in Fig. 5(a). If θ is kept fixed, for example at 45°, the LS appear for any value of $q_b \gtrsim 0.9$. The upper boundary of the existence region goes down for increasing q_b. For $0.9 \lesssim q_b \lesssim 1.3$ the transition to LS occurs starting from an upper state more or less regularly patterned by hexagons; at $q_b \gtrsim 1.3$ the patterned state from which LS emerge for decreasing I_0 is of space–time chaotic nature. The lower boundary, below which a transition to homogeneous state occurs, goes up for decreasing q_b. This is a consequence of the fact that LS have an internal structure containing both low and high frequency components. Therefore, any bandwidth limitation perturbs the LS structure, and increases the threshold for their existence.

Let us now consider the dependence on θ of (q_b, I_0) sections. For any value of θ the region of existence of LS has qualitatively similar contours to the ones above described, but its area decreases monotonically when departing from $\theta = 45°$. Ultimately, at a lower limit of $\theta \simeq 38°$ and at an upper limit of $\theta \simeq 54°$, localization is no more observed. This dependence is related to the range ΔI_0 at which bistability between uniform and patterned branches exists.[12] Indeed, ΔI_0 has a maximum at $\theta = 45°$, where the interference term

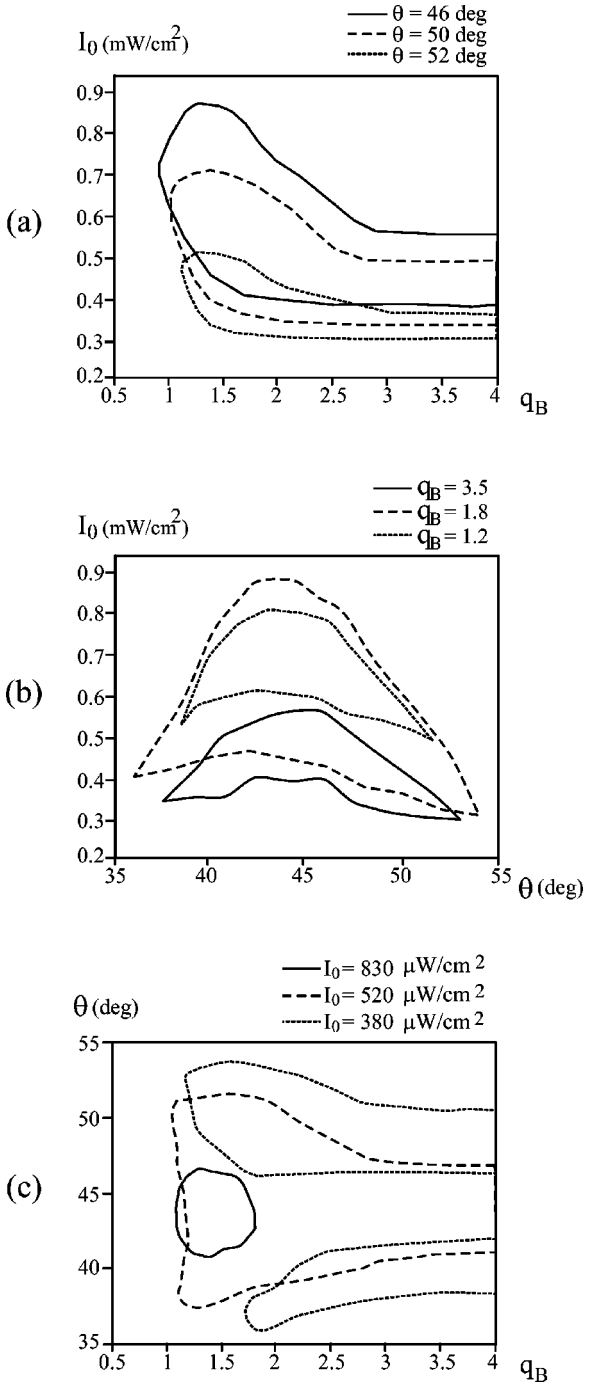

FIG. 5. Sections of the LS existence volume parallel to (q_b, I_0) (a), (θ, I_0) (b), (q_b, θ) (c).

BC in the feedback is maximum, and decreases while departing from this value.

The dependence of the volume of existence of LS in the planes parallel to (θ, I_0) is of the kind displayed in Fig. 5(b). The shape and location of this area is independent of q_b for $q_b \gtrsim 3.5$. This is a consequence of the fact that spatial frequencies higher than this value are absent in the single LS spectrum, which is now limited by the LCLV diffusion length $l_d \simeq 30\ \mu$m.

When q_b is decreased starting from this asymptotic value, the existence region of LS in the planes parallel to

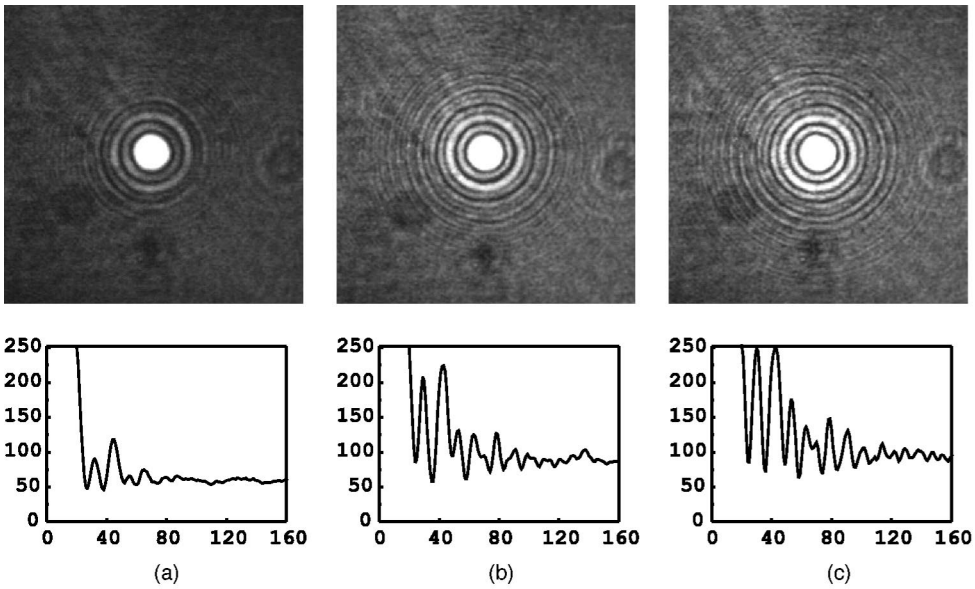

FIG. 6. Pictures and radial profiles (averaged on the azimuthal coordinate) of the localized structures, for increasing intensity. $I_0=360\ \mu\mathrm{W/cm^2}$ (a); $I_0=530\ \mu\mathrm{W/cm^2}$ (b); $I_0=620\ \mu\mathrm{W/cm^2}$ (c). The other parameters are fixed at $\theta=45°$, $q_b=4$, $\varphi_0=1.09\ \pi$.

(θ,I_0) maintains a similar shape, but moves towards higher values of I_0 and widens, reaching a maximum area for $q_b \simeq 1.8$. This dependence arises from the fact that a decrease of q_b from its asymptotic value corresponds to a cutoff of some spatial frequencies; these are the ones that lose stability at high values of I_0 in the case of very large q_b, thus limiting the existence range of localized structures.

If q_b is further decreased to values $\lesssim 1.8$, the region of LS existence in the planes parallel to (θ,I_0) still moves towards higher values of I_0, but now its area shrinks, until, at $q_b \simeq 1$, localization is no more observed. In this regime, cutting of spatial frequencies clearly has a destructive role on the possibility of LS existence.

In the planes parallel to (q_b,θ), finally, the sections of the LS existence volume have the shape shown in Fig. 5(c). At high intensities the occurrence of localization is observed only for a limited range of q_b; outside this range, instabilities of high frequency components lead to extended patterns belonging to the upper branch. When I_0 is decreased, this phenomenon no longer limits the existence of LS, that consequently are observed up to arbitrarily large values of q_b. At the same time, the range of localization along θ widens.

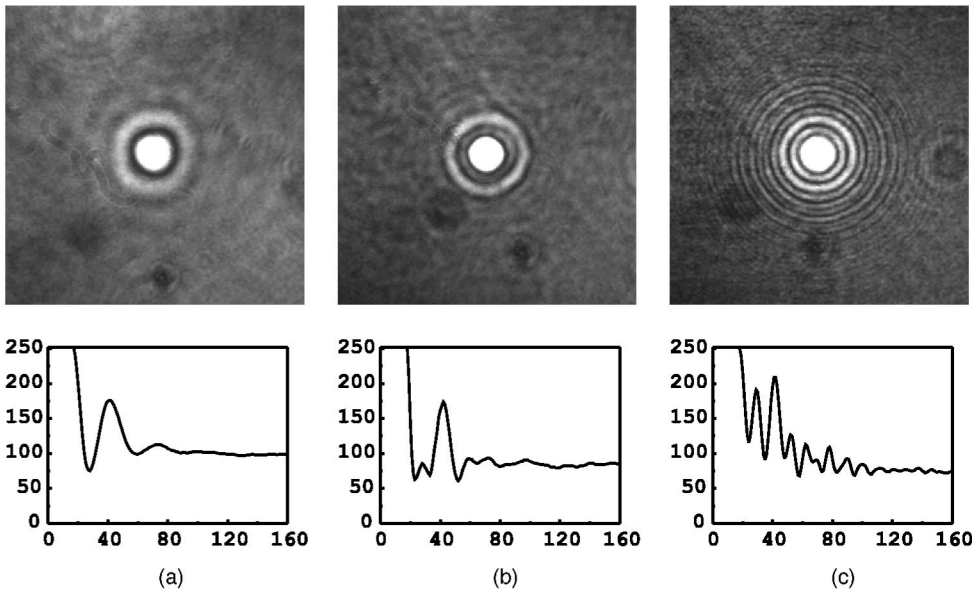

FIG. 7. Pictures and radial profiles of the localized structures, for increasing spatial bandwidth q_b. $q_b=1.1$ (a); $q_b=2.0$ (b); $q_b=4.0$ (c). The input intensity is set to a value lying approximately at the center of the existence range of LS for any value of q_b. The other parameters are fixed at $\theta=45°$, $\varphi_0=1.09\ \pi$.

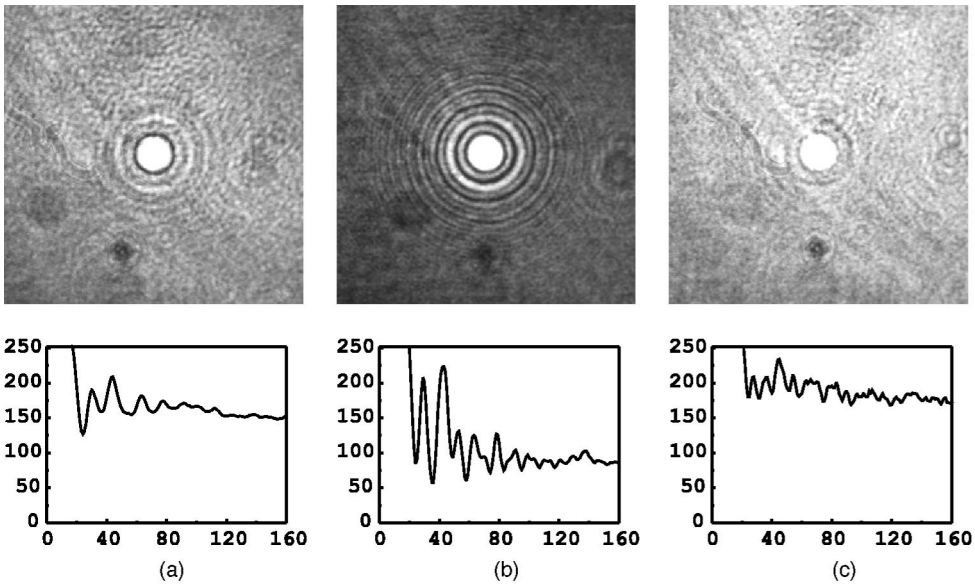

FIG. 8. Pictures and radial profiles of the localized structures, for increasing angle θ. $\theta=38°$ (a); $\theta=45°$ (b); $\theta=54°$ (c). The input intensity is set to a value lying approximately at the center of the existence range of LS for any value of θ. The other parameters are fixed at $q_b=4$, $\varphi_0=1.09\ \pi$.

At even smaller intensity values a region is seen in which LS exist only for θ lying in two distinct bands, which shrink for decreasing I_0, leaving eventually the lower uniform state as the only stable configuration.

IV. CONTROL OF THE LOCALIZED STRUCTURES PROPERTIES

The several parameters discussed in the previous section have an important influence in determining not only the existence range of the LS, but also their spatial shape. As a consequence, it is possible to broadly tune the properties of the structures acting on one or more of these variables. Figure 6 shows the dependence of the LS profile upon the intensity I_0, keeping fixed the other parameters (see figure caption for their values). It is apparent that the main effect of an increase of I_0 consists in a corresponding increase of the amplitude of the oscillations on the LS tails. Aside from this, a slight monotonic variation of both the lower and the upper intensity levels is observed. This last one is not visible in the figures presented, since they are saturated in order to allow visualization of low intensity details.

It has been recognized[16,11] that the oscillations on the tails are responsible for the interactions between LS, leading eventually to the formation of bound states of the kind shown in Fig. 2. In particular, it has been predicted that the force exerting between a pair of LS is of oscillatory sign as a

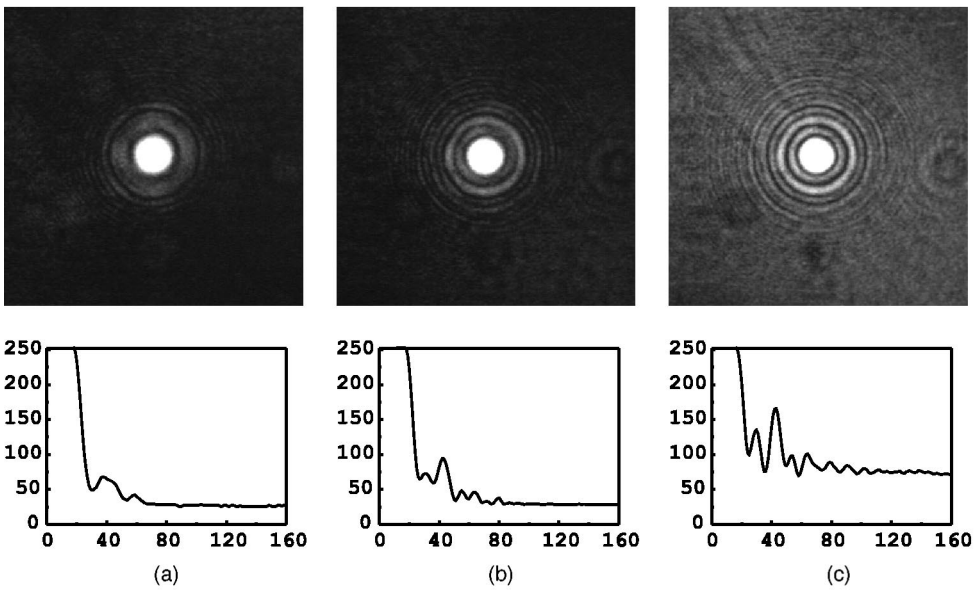

FIG. 9. Pictures and radial profiles of the localized structures, for increasing angle φ_0. $\varphi_0=\pi$ (a); $\varphi_0=1.03\ \pi$ (b); $\varphi_0=1.07\ \pi$ (c). The other parameters are fixed at $\theta=45°$, $I_0=580\ \mu\mathrm{W/cm}^2$, $q_b=4$.

function of their mutual distance, with a periodicity given by the wavelength of the oscillations on each LS tail. It is also expected that the strength of these forces be proportional to the amplitude of these oscillations.

In Ref. 25 we have investigated how the forces between LS depend on the tail features. Precisely, the wavelength of the LS tails was varied using q_b as a control parameter. As shown in Fig. 7, increasing q_b induces an increase of this wavelength, and ultimately an asymptotic constant value is reached for $q_b \simeq 3.5$. Accordingly, we have observed that the average distance between pairs of localized structures in a bound state corresponds very closely to the q_b-tuned wavelength on the single LS tail.

Following the definitions of B and C in Eqs. (4) and (5), we see that a variation of the angle θ affects the values of both the interferential and the diffractive contributions to the feedback intensity. Since these phenomena are responsible for the selection and stability of the two branches involved in the LS formation, it is expected that variations of θ greatly affect the features of the observed solitons. Figure 8 shows how the shape of the structures modifies as θ varies across the range in which localization is observed. Two main effects of the variation of θ appear here. On one side, due to the tuning of the interferential contribution, the intensities of the lower and upper branches are strongly dependent on θ. Thus, bright solitons on a very dark background are observed at $\theta \simeq 45°$, while the intensity difference between the involved branches decreases noticeably at the extrema of the range of localization ($\theta \simeq 38°$, $\theta \simeq 54°$). Specifically, the ratio $I_{\text{peak}}/I_{\text{background}}$ varies from a maximum of $\simeq 10$ at $\theta = 45°$, to a minimum of $\simeq 4$ at $\theta = 54°$. On the other side, the amplitude of the oscillations on the tails is also affected by the value of θ, displaying a clear maximum at $\theta = 45°$. Accordingly to the previous discussion, this suggests the use of θ as a parameter for tuning the interaction strength between pairs of LS.

Let us finally consider the effect on LS of the phase angle φ_0, experimentally controlled via the external voltage applied to the LCLV. Figure 9 reports the solitons observed for increasing values of φ_0, starting from $\varphi_0 = \pi$. A first, very clear effect is the modification of the contrast between dark and bright states involved in the formation of the structure. As expected from a qualitative analysis of Eqs. (3)–(5), the maximum contrast is obtained for $\varphi_0 = \pi$, at any value of θ. Tuning the LS contrast using this parameter can be of interest in view of applications, in which these solitons are used as pixels for the storage and/or the processing of optical information.

Besides this effect on contrast, the variation of φ_0 also influences amplitude and wavelength of the LS tails (see Fig. 9). This is not surprising, since it is clear from an inspection of the system equations that φ_0 affects the selection of the unstable as well as the weakly stable scales. These last ones are actually those observed in the tails, connecting the stable uniform lower branch to the upper patterned one. A clear and quantitative understanding of the role of φ_0 on the selection of the tail properties has nevertheless not yet been achieved at the moment of writing.

ACKNOWLEDGMENTS

The authors acknowledge E. Benkler, L. Pastur, and S. Ducci for many fruitful discussions. Work partly supported by EEC Network No. HPRN-CT-2000-00158.

[1] M. Cross and P.C. Hohenberg, Rev. Mod. Phys. **65**, 851 (1993).
[2] F.T. Arecchi, S. Boccaletti, and P.L. Ramazza, Phys. Rep. **318**, 1 (1999).
[3] Journal of Optics B, Quantum and Semiclassical Optics, Vol. **2**, 2000, Papers from the 2nd Euroconference on Trends in optical nonlinear dynamics (COCOS '99) on complex behaviour in optical systems and applications, edited by W. Lange and T. Ackemann.
[4] For a review, see, e.g., H. Riecke, *Localized Structures in Pattern-Forming Systems*, in *Pattern Formation in Continuous and Coupled Systems*, edited by M. Golubitsky, D. Luss, and S. Strogatz (IMA Springer, Berlin, 1999), Vol. 115, p. 215.
[5] E. Moses, J. Fineberg, and V. Steinberg, Phys. Rev. A **35**, 2757 (1987).
[6] H.H. Rotermund, S. Jakubith, A. Von Oertzen, and G. Ertl, Phys. Rev. Lett. **66**, 3083 (1991).
[7] P. Umbanhowar, F. Melo, and H. Swinney, Nature (London) **382**, 793 (1996).
[8] M. Saffman, D. Montgomery, and D.Z. Anderson, Opt. Lett. **19**, 518 (1994).
[9] V.B. Taranenko, K. Staliunas, and C.O. Weiss, Phys. Rev. Lett. **81**, 2236 (1998).
[10] A. Schreiber, B. Thuring, M. Kreuzer, and T. Tschudi, Opt. Commun. **136**, 415 (1997).
[11] B. Schapers, M. Feldmann, T. Ackemann, and W. Lange, Phys. Rev. Lett. **85**, 748 (2000).
[12] P.L. Ramazza, S. Ducci, S. Boccaletti, and F.T. Arecchi, J. Opt. B: Quantum Semiclassical Opt. **2**, 399 (2000).
[13] V.B. Taranenko, I. Ganne, R.J. Kuszelewicz, and C.O. Weiss, Phys. Rev. A **61**, 063818 (2000).
[14] J. Tredicce, Communication at the Sixth Experimental Chaos Conference, Potsdam, Germany, 2001.
[15] Y. Pomeau, Physica D **23**, 3 (1986).
[16] I.S. Aranson, K.A. Gorshkov, A.S. Lomov, and M.I. Rabinovich, Physica D **43**, 435 (1990).
[17] D. Bensimon, B.I. Shraiman, and V. Croquette, Phys. Rev. A **38**, 5461 (1988).
[18] P. Coullet, C. Riera, and C. Tresser, Phys. Rev. Lett. **84**, 3069 (2000).
[19] M.A. Vorontsov, M.E. Kirakosyan, and A.V. Larichev, Sov. J. Quantum Electron. **21**, 105 (1991).
[20] S.A. Akhmanov, M.A. Vorontsov, V. Yu. Ivanov, A.V. Larichev, and N.I. Zheleznykh, J. Opt. Soc. Am. B **9**, 78 (1992).
[21] F.T. Arecchi, S. Boccaletti, S. Ducci, E. Pampaloni, P.L. Ramazza, and S. Residori, J. Nonlinear Opt. Phys. Mater. **9**, 183 (2000), and references therein.
[22] E. Yao, F. Papoff, and G.L. Oppo, Phys. Rev. E **59**, 2918 (1999).
[23] H. Sakaguchi and H.R. Brand, Europhys. Lett. **38**, 341 (1997).
[24] R. Neubecker, G.L. Oppo, B. Thuering, and T. Tschudi, Phys. Rev. A **52**, 791 (1995).
[25] P.L. Ramazza, S. Boccaletti, U. Bortolozzo, S. Ducci, E. Benkler, and F.T. Arecchi, Phys. Rev. E **65**, 066204 (2002).